Efficient Degradation of Fenitrothion Pesticide and Reaction Mechanism with GO-Fe_3O_4/TiO_2 Mesoporous Photocatalyst under Visible Light Irradiation

Mostafa Zangiabadi (MSc)[1,2], Asma Saljooqi (PhD)[1,2], Tayebeh Shamspur (PhD)[1], Ali Mostafavi (PhD)[1], Fatemeh Mehrabi (MSc)[1,2], Maryam Mohamadi (PhD)[3*]

[1] *Department of Chemistry, Shahid Bahonar University of Kerman, Kerman, Iran*
[2] *Young Research Society, Shahid Bahonar University of Kerman, Kerman, Iran*
[3] *Pistachio Safety Research Center, Rafsanjan University of Medical Sciences, Kerman, Iran*

Information

Article Type:

Original Article

Article History:

Received: 22 Jan. 2019
Accepted: 10 Mar. 2019
DOI: 10.22123/phj.2019.170505.1027

Keywords:

GO-Fe_3O_4/TiO_2 Nanocomposite
Pesticide
Fenitrothion
Photocatalyst
Mesoporous Material

Corresponding Author:

Maryam Mohamadi

Email: m.mohamadi794@gmail.com

Tel: +98 34 34282705

Abstract

Introduction: Fenitrothion is one of the common pesticides used in pistachio orchards. Although strict rules have been laid down for the use of sustainable organic pollutants, they are still detected in natural water.

Methods: In this work, highly ordered mesoporous titanium dioxide (TiO2 mesoporous) with large pore size and high surface area, iron (II, III) oxide nanoparticles (Fe3O4) and graphene oxide (GO) was successfully fabricated and GO-Fe3O4/TiO2 (GFT) mesoporous nanocomposite proposed as a heterogeneous photocatalyst. The physicochemical and morphology, properties of GO-Fe3O4/TiO2 mesoporous were characterized by field emission scanning electron microscopy with energy dispersive X-Ray spectroscopy (FESEM-EDS), transmission electron microscopy (TEM), X-ray diffraction (XRD), and specific surface area by the BET method.

Results: The GO-Fe3O4/TiO2 mesoporous showed a good photocatalytic activity for the degradation of fenitrothion, achieving almost complete removal of 6 ppm fenitrothion after 60 min contact with 0.06 g/L of the nanocatalyst in nutral pH. The degradation of fenitrothion was found to follow the pseudo-first order according to kinetic analysis.

Conclusion: GO-Fe3O4/TiO2 mesoporous is a recyclable catalyst that effectively degrade fenitrothion pesticide in aqueous media.

►Please cite this article as follows:

Zangiabadi M, Saljooqi A, Shamspur T, Mostafavi A, Mehrabi F, Mohamadi M. Efficient degradation of fenitrothion pesticide and reaction mechanism with GO-Fe3O4/TiO2 mesoporous photocatalyst under visible light irradiation. Pistachio and Health Journal. 2019; 2 (1): 10-21

1. Introduction

Some of the common pesticides used in agriculture, especially pistachio gardens are fenitrothion, Imidacloprid, Diazinon, Phosalone, and Chlorpyrifos [1]. Asia is the largest pesticide consumer in the world after Europe [2, 3]. Although strict rules have been laid down for the use of sustainable organic pollutants, they are still detected in natural water [4]. About 50% of these pollutants penetrate water, soil, living creatures, and other sources [5].

It has been reported that FT[1] contamination also affects microorganisms and plant enzymes [6].

Numerous studies have established that TiO_2 as a photocatalyst in the form of nanoparticles is much more efficient than in bulk powder [7]. When the semiconductor radius reaches its critical radius (about 10 nm), each charge carrier behaves quantum mechanically [8]. The mesoporous of TiO_2 is one of the structures used for photocatalytic work under visible light and ultraviolet irradiation since the band gaps are in the range of the wavelength both the visible and the ultraviolet light [9]. It has been determined that this photo catalytic activity is highly dependent on its surface area, the synthesis method, and the crystalline structure [10]. The mesoporous TiO_2 was first synthesized by using a template-directing approach. This method has taken its place since using the supra molecular assembly theory [11]. Recently, non-magnetic and magnetic nanoparticles have been synthesized in different methods for catalytic and other applications. Iron, nickel, and cobalt oxides show magnetic properties [12, 13]. In this study, GO-Fe_3O_4/TiO_2 mesoporous (GFT) were synthesized by the template-based and hydrothermal method.

In general, pores are divided into two categories. The pores are closed individually; however, the open pores are connected to each other. Open-pore materials are more practical than closed ones. The IUPAC[2] classification of the porous material based on size is divided into three categories, microporous (L< 2nm), mesoporous (2< L <50nm), and macroporous (L> 50nm); L is pore diameter. Further, based on the crystalline framework and structural ordering, they are divided into three general categories: inorganic-organic mixtures, purely inorganic, and all carbon materials, which are naturally porous [14- 16].

The material discovery of the mesoporous in early 1990 and its other derivatives coincided with the development of material engineering [17]. In the synthesis, the molding mechanisms can differ depending on the synthesis conditions of the source, as well as the type of surfactant used [18]. Pesticides are considered to be hazardous to human health, and demand for them is high [19]. In a study on rats in several laboratories, the World Health Organization has examined pesticide toxicity [20]. Pesticides are classified into 4 categories based on their chemical structure and toxicity level [21, 22].

Class I (Organochlorine): These types of pesticides are very stable in the environment

[1] Fenitrothion (FT)

[2] International Union of Pure and Applied Chemistry (IUPAC)

and can penetrate the adipose tissue. The mainstay of them is to eradicate diseases, such as malaria and dengue. They are used for the cultivation and maintenance of lettuce, tomatoes, rice, cotton, alfalfa, corn, and grapes. In humans, it mainly causes a disorder in the nervous system, as well as a change in the kinetic flow of Na^+ and K^+ions in the membrane of the nerve cells by changing the cell membrane that ultimately causes symptoms, such as seizures and acute poisoning, and death from respiratory arrest [23, 24].

Class II (Organophosphates): These compounds are derived from phosphoric acid. In humans, it affects the central nervous systemby disabling the acetylcholinesterase enzyme (which transmits acetylcholine), and with phosphorylation active hydroxyl groups, the active sites of enzymes disrupt nerve stimulation, including symptoms like headache, dizziness, seizure, nausea, loss of reflexes, coma, and even death. This group of pesticides is also very important in terms of leakage because it can directly react with alkyl, ethyl, and nitrogen groups with electrophilic and nucleophilic succession reactions. These pesticides are used in herbal products, fruit gardens, sugar cane, cotton, and cereals [25, 26].

Class III (Carbamates): These compounds are esters derived from dimethyl N-methylcarbamic acid, which are used as fungicides of insecticide herbicides and nematicides. The stability of these compounds is less than organophosphate and organochlorine. It can also inhibit the acetylcholine stars enzyme. Consequently, it quickly acts by reacting with electrophilic groups and steric carbamoyl, as well as blocking the position of enzymes [27].

Class IV (Pyrethroids): These types of pesticides can be obtained from the Pyrethrum of chrysanthemum flower extract synthesized later artificially. At present, more than 100 commercial products are produced for various purposes. They act on the central nervous system, causing changes in the dynamics of the Na^+ channels in the nerve cell membrane; this, inturn, leads to increase its opening time, prolonging sodium current across the membrane in both vertebratesandinsects [28].

2. Materials and Methods

2.1. Synthesis of the TiO_2 Mesoporous

All the chemicals used in this experiment were from Sigma-Aldrich, USA. TiO_2 mesoporous were prepared via template-based methods. Pure ethanol and HCl (37%) mixed under the magnetic stirring condition for 5 min. TTIP[3] drops were added to the solution to make the solution clear. 0.64 mL of acetylacetone was added as well.

The TiO_2 solution was kept under magnetic stirring for 20 min. 0.63g of F127 was added to 5mL of pure ethanol. The obtained clear solution was added to the TiO_2 solution, and it was stirred for 3h. The solution was transferred to a glass dish and dried at 120°C for 24h.The white powders were placed in the furnace for 4h in order to remove the template.

2.2. Synthesis of Fe3O4 Nanoparticles

The preparation of Fe_3O_4 magnetic nanoparticles was based on mixing $FeCl_2.4H_2O$ (0.5g) and $FeCl_3.6H_2O$ (1.37g) in

[3] Titanium Tetra Iso Propoxide (TTIP)

120mL of distilled water that had been freshly boiled to expel CO_2. Then, this solution was stirred with a mechanical stirrer (800 rpm) at 60°C for 30 min. Owing to the presence of oxygen in the atmosphere, nitrogen gas was continuously injected into the solution. Following that, 11 mL of 25% NH_3 was constantly added to the solution. The magnetite precipitates were collected by a magnet and washed several times with distilled water. Finally, they were dried in an oven at 90°C for 10 h and kept for reuse in the 0°C.

2.3. Synthesis of GFT photocatalyst

After the preparation of GO [29], to prepare GFT, 30 mg GO and 20 mg Fe_3O_4 added to 200 mL of distilled water, and it was stirred severely at 50°C. 300 mg of TiO_2 mesoporous was dispersed into 50 mL of distilled water sonicating for 10 min to form a stable TiO_2 mesoporous suspension. Subsequently, these produced nanoparticles were slowly added to magnetic nanoparticles of Fe_3O_4 for 5 min. After all these treatments, the suspension was refluxed at 50°C for 24 h, and it was cooled atroom temperature. Finally, GFT photocatalysts were collected by external magnet and then washed with ethanol and distilled water.

2.4. Photocatalytic Degradation Experiments

The FT solution was mixed with a specific amount of photocatalyst, and the photocatalytic process was performed. Before the test, the solution was placed in the dark at room temperature to ensure photocatalytic properties. Irradiation was carried out using a visible lamp. The radiation was performed by a visible light lampmainly in the wavelength range of 400-700nm. After a certain period, the photocatalysts were separated by an externalmagnet, and the solution was analyzed by the UV-Vis[4] spectrometer. Degradation of FT rates was compared before and after the visible irradiation.

3. Results and Discussion

3.1. Characterization

The surface properties of fresh and used samples were measured by N_2 adsorption calculated using BET[5] and BJH[6]. The size distribution curve clearly showed that the synthesized material had unique mesoporous channels. Based on the calculation of the linear part of the BET plot (Fig. 1a), the surface area of pure TiO_2 was 834.48 m^2 g^{-1}, and pore volume of 1.1266 cm^3 $g^{-1}$was high as compared to other research results [30, 31]. Fig. 1b shows N_2 adsorption-desorption isotherm and pore size distribution of the TiO_2 mesoporous. The mean pore diameter of this nanocatalyst is 5.4 nm. These indicate that the mesoporous structures have the best surface for their application in photocatalyst with high efficiency and degradation power.

To study the structural properties of TiO_2 mesoporous, the GFT mesoporous was analyzed using TEM. The nanoporous structure of the gifts clearly was displayed on their TEM[7] images in Fig. 2A. In the TEM image of the sample, the mesoporous structure like a fingerprint can be observed. Fig. 2B shows an SEM[8] image of prepared GFT

[4] Ultrviolet-Visible (UV-Vis)
[5] Brunauer Emmett Teller (BET)
[6] Barret Joyner Halender (BJH)
[7] Scanning Electron Microscope (TEM)
[8] Scanning Electron Microscope (SEM)

mesoporous nanocatalyst. In this Fig, an agglomeration of nearly spherical particles is observed. A typical EDAX[9] pattern of this nanocatalyst is given in Fig. 2C; to characterize the elemental composition of the GFT mesoporous nanocatalyst, EDAX analysis is used. The final nanocomposite contains all of the elements, i.e., Ti, O, Fe, and C.

To investigate crystal structures, XRD[10] analysis was done. The XRD pattern of TiO_2 was displayed in Fig. 3A sharp peak at 31.8◦C was related to the TiO_2 mesoporous sample. This was due to the high temperature of calcination. Practically, the wide width of the peaks demonstrated small crystallite size, which was estimated to be about 5.7 nm using the Debye-Scherer equation. In this pattern, all three forms of anatase, rutile, and brookite were shown. These results are in good agreement with the SEM results. It is worth to note that the crystalline size is in the range of 4.4-9.6 nm, which is known to be optimized for high photocatalytic activity.

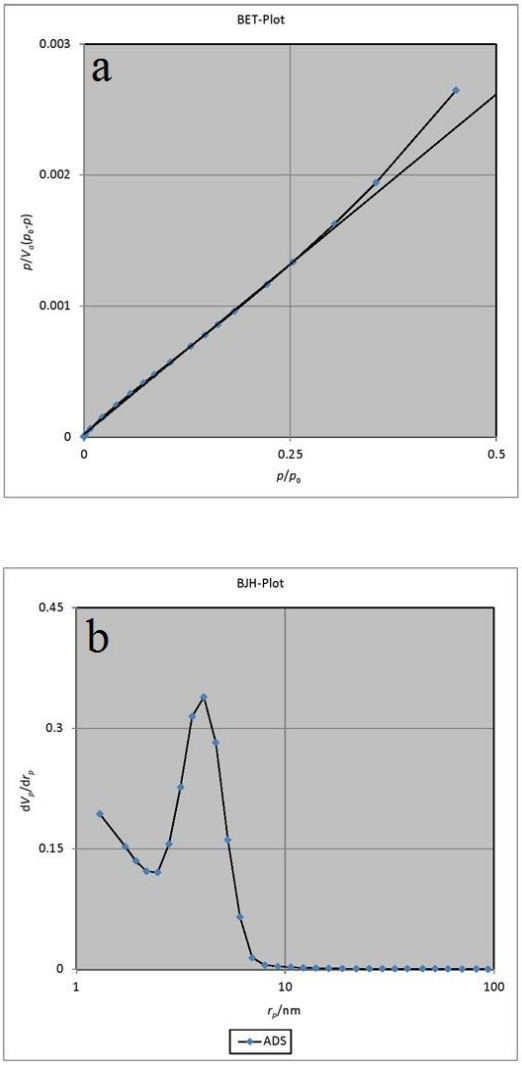

Fig. 1. Nitrogen adsorption and desorption isotherms of GFT nanocompositeand (b) The pore size distributions of GFT nanocomposite

[9] Energy-Dispersive X-ray Spectroscopy (EDAX)
[10] X-ray Powder Diffraction (XRD)

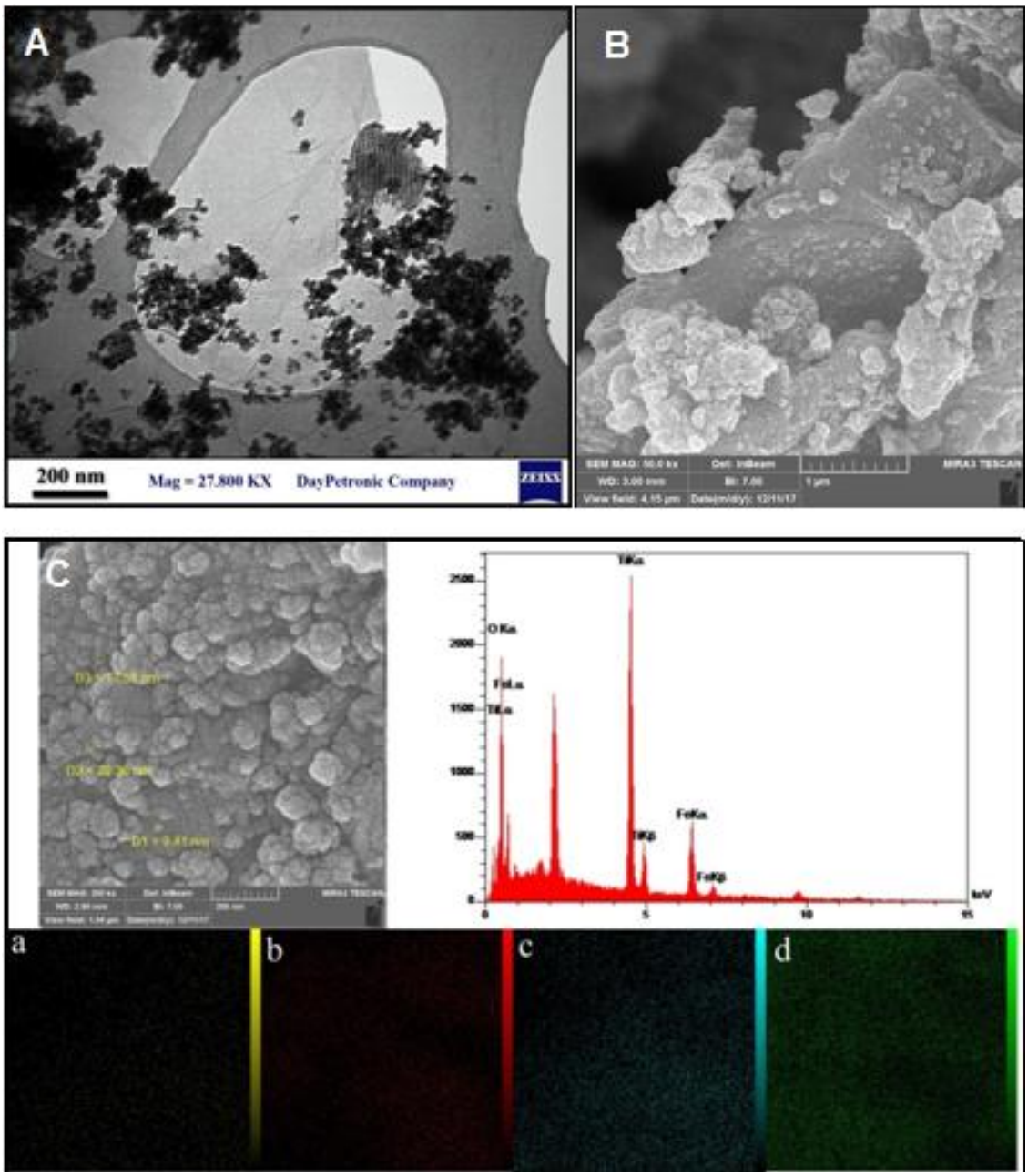

Fig. 2. (A) TEM image of the GO-Fe_3O_4/TiO_2 mesoporous nanocomposite, (B) FE-SEM image of the GO-Fe_3O_4/TiO_2 mesoporous nanocomposite, and (C) EDX analyses of GO-Fe_3O_4/TiO_2 mesoporous nanocomposite

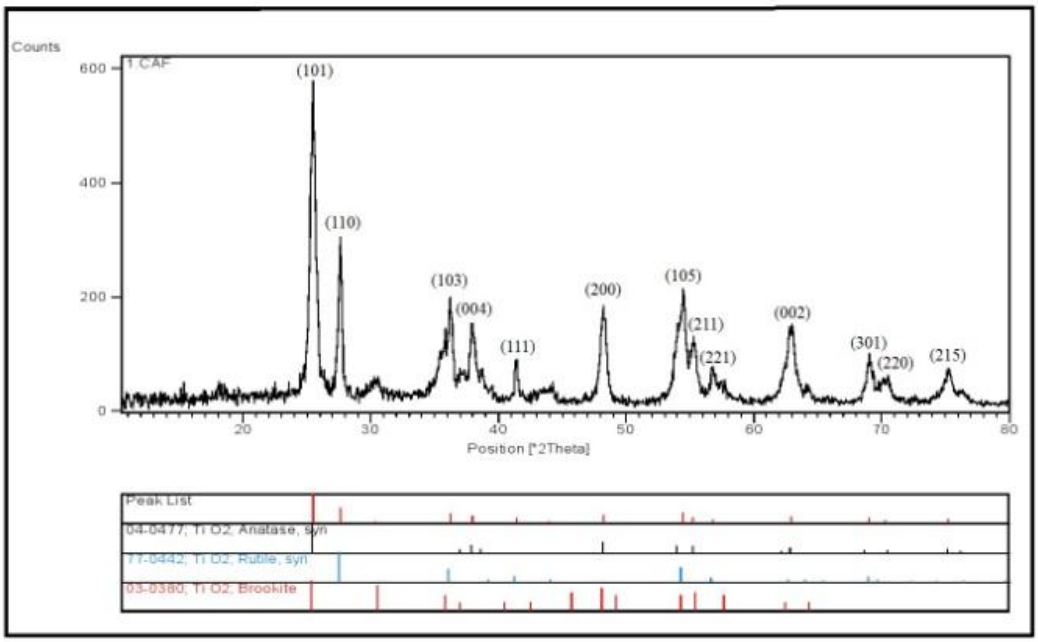

Fig. 3. XRD patterns for TiO2mesoporous

3.2. Photocatalytic Degradation of FT

3.2.1. Effect of Initial FT Concentration

The effect of FT concentration on the degradation rate was considered within the range of 2 to 10 ppm at a GFT nanocatalyst dose of 0.4 g. The photocatalytic degradation efficiency of FT showed a decrease by an increase in the FT concentration, and the highest photocatalytic degradation was observed at 4 ppm of the FT concentration (Fig. 4a).

3.2.2. Effect of Catalyst Dose

The effect of catalyst amount on the efficiency of FT degradation was investigated, ranging from 0.1 g to 0.6g. As shown in Fig. 4b, the degradation percentage of FT pesticide rose with raised catalyst amount, and it was selected as optimum in 0.4 g. With increasing the amount of FTG, the numbers of FT molecules absorbed on the surface of the catalyst and visible light photons increased, increasing the rate of photodegradation reaction. High doses of the photocatalyst caused a decrease in the diffusion of visible light; hence, photodegradation of suspension decreased.

3.2.3. Effect of Illumination Time

The results of the illumination time were shown in Fig. 4c. According to these results, the photocatalytic performance of FT degradation raised with an increase in time from 10 to 70 min. The degradation reaction of pesticide happened on the surface of GFT. Visible light created electron-hole pairs on the GFT catalyst surface, and superoxide radical ions (O_2^-) were formed. Also radicals HO was produced from the H_2O reaction at the nanocatalyst surface. The oxidizing ability of

HO was significant enough to completely oxidize FT adsorbed on the surface of nanocatalyst into NO_2^-, SO_4^{2-}, CO_2, H_2O, and other mineral compounds [32]. As seen in Fig. 4c, the degradation efficiency increases significantly up to 50 minutes. However, after 50 minutes, the degradation efficiency is not significantly increased due to reduced formation of radicals HO.

3.2.4. Effect of pH

The effect of pH in the photocatalytic reactions is very essential. The influence of pH on the percentage of photocatalytic degradation was examined (range 3-12) at 6 ppm FT concentration with 0.4 g of GFT. The pH changed influence on the adsorption of molecules considerably at the photocatalyst surface. The hydroxyl radicals were formed at the GFT nanocatalyst surface and reacted with the holes. The holes supplied the oxidation sites at low pH. In the basic media, hydroxyl radicals were simply formed near the nanocatalyst surface. The low efficiency in pH=4 was due to the dissolution of the catalyst in acidic conditions (Fig. 4d).

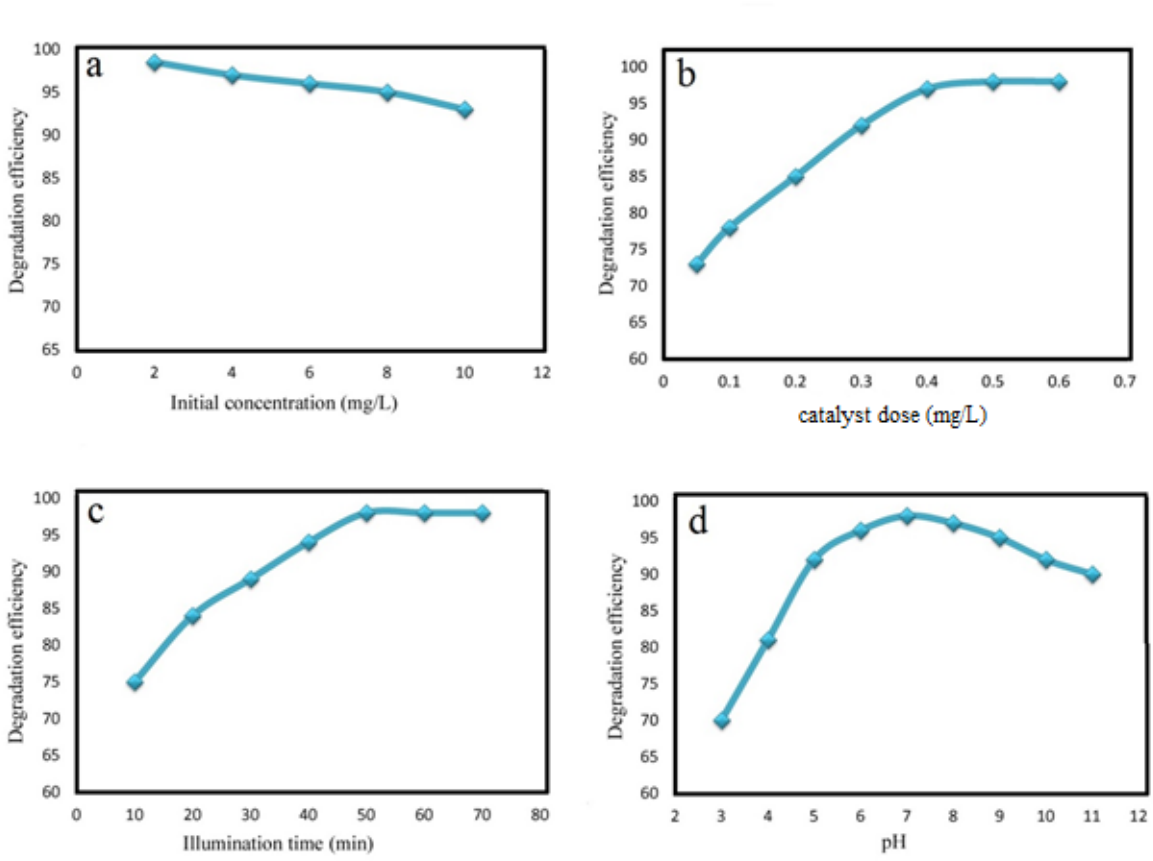

Fig. 4. Effect of various parameters (a) initial concentration (b) GTF dose (c) illumination time and (d) pH on the degradation of FT

3.2.5. Reusability

The GFT nanocomposite was isolated easily from the solution using an external magnet, and it was used for the next cycle. To test the catalyst reusability, a catalytic amount was used successively 7 times. GFT nanocomposite can be recycled and reused 7 times without losing efficiency. This shows that the adsorptive and photocatalytic properties of FTG nanocomposite is stable, which is an essential matter. The reusability of GFT nanocomposite is shown in Fig. 5. The variation of FT concentrations was determined using a UV–Vis spectrometer with absorbance in the range of 200 to 800 nm.

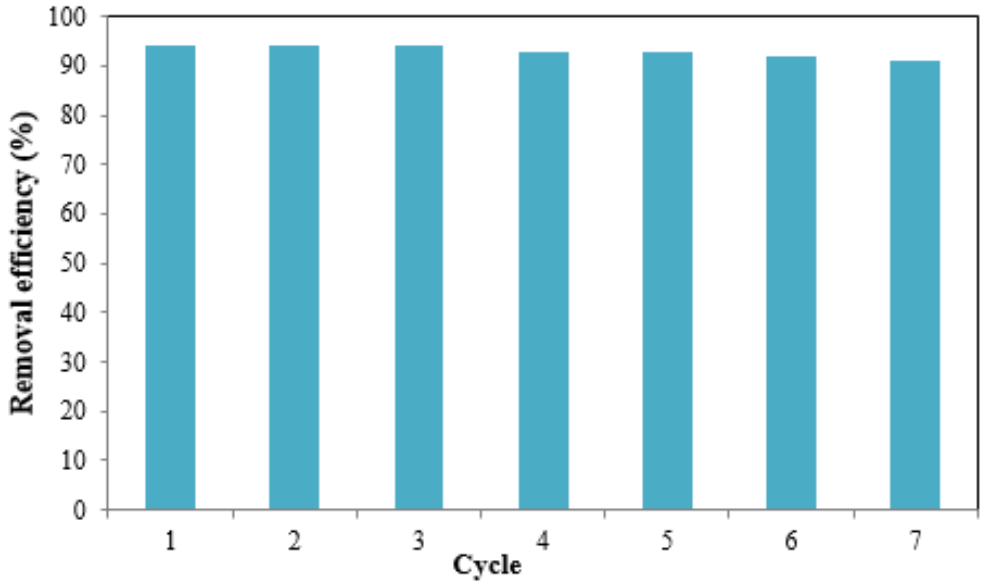

Fig. 5. Degradation of FT in different batch runs in the GO-Fe_3O_4/TiO_2 mesoporous system

3.2.6. Kinetics of FT

The kinetics of the photocatalytic reactions were defined using the first-order kinetic model as follows:

$$\mathrm{Ln}\left(\frac{C_t}{C}\right) = -kt$$

Where C is the initial FT concentration, and $C_t$isFT concentration at t moment (Langmuir–Hinshelwood model) [32]. By plotting the Ln(C_t/C) diagram versus t, the lines are drawn approximately straight (Fig. 6). This implies that the degradation of FT is followed as pseudo-first-order kinetic.

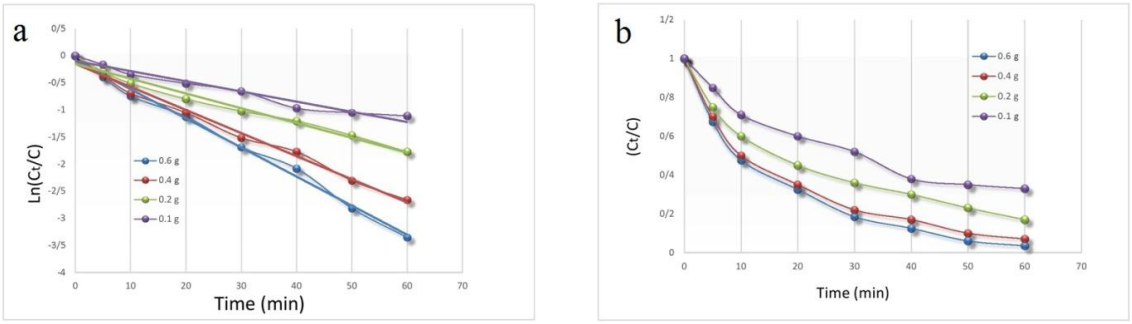

Figu. 6 (a) The effect of catalyst amount on the photocatalytic degradation of FT and (b) the linear plot fitting of the pseudo-first-order kinetic model

4. Conclusion

TiO_2 mesoporous have been synthesized by a template-based method using F127 polymer and titanium tetra isopropoxide as the source materials. TiO_2 mesoporous and Fe_3O_4 successfully were placed on the Graphene oxide substrate. Fenitrothion pesticide in aqueous phase could be successfully degraded in a GO/Fe_3O_4-TiO_2 mesoporous suspension under visible solar light irradiation. The porosity of TiO_2 photocatalyst showed a maximum degradation of 97% visible light. This enhanced photocatalytic activity could be attributed two forms of anatase and rutile TiO_2 (according to the XRD analysis) and retarded fast electron-hole pair recombination by doping the catalyst with Fe_3O_4 and GO. BET and BJH plots for TiO_2 mesoporous showed that surface area and pore volume as 834.48 m^2/g and 1.1266 cm^3/g, respectively. The results indicated that under optimum conditions of GFT 0.6 g/L, 4 ppm, pH: 7, and reaction time 60 min, the photocatalyst presented the maximum removal efficiency. The kinetic analysis of FT photodegradation followed pseudo-first-order kinetics, according to Langmuir-Hinshelwood model. Further, the findings showed that the new GO-Fe_3O_4-TiO_2 mesoporous photocatalyst could be efficiently used for water treatment, and the catalyst particles could be easily removed from the system using external magnet. Finally, the application of the GFT photocatalyst in Fenitrothion pesticide degradation on environmental water samples (bore well, river, pond, and dam) was tested; it showed its worthy performance in the purification of the water.

Conflict of interest

The authors declare no conflicts of interest.

Acknowledgments

The authors would like to express their sincere appreciationto Mr. Alireza Afzalipour for his foresight and generosity in establishing Kerman University to train future generations of doctors, engineers, scientists and educators. In additions the authors hereby acknowledges his/her thanks to Dr. Dabiri for his generous support the activities of the chemistry laboratories in Kerman University. Some of the project funding was supplied by the Rafsanjan University of Medical Sciences (RUMS). This study was approved by the RUMS ethical committee by the number of IR.RUMS.REC.1397.133.

References

1. Rezg R, Mornagui B, El-Fazaa S, Gharbi N. Organophosphorus pesticides as food chain contaminants and type 2 diabetes: a review. Trends in food science & technology. **2010**;21: *345-357*.
2. Zhang W, Jiang F, Ou J. Global pesticide consumption and pollution: with China as a focus. Proceedings of the International Academy of Ecology and Environmental Sciences. **2011**;1: *125-144*.
3. Faraji M, Noorbakhsh R, Shafieyan H, Ramezani M. Determination of acetamiprid, imidacloprid, and spirotetramat and their relevant metabolites in pistachio using modified QuEChERS combined with liquid chromatography-tandem mass spectrometry. Food chemistry. **2018**;240:*634-641*.
4. Loos R, Gawlik BM, Locoro G, Rimaviciute E, Contini S, Bidoglio G. EU-wide survey of polar organic persistent pollutants in European river waters. Environmental Pollution. **2009**;157: *561-568*.
5. Dehghani R, Dadpour B, Mirza Mohhamadi S, Ebnerasol F, Froghi M, Jalali Z, Moghimipour M, Lajevardi M, Malekzadeh H, Vaziri M. Pesticide Consumption in Greenhouses; a Case Study of Kashan Region. International Archives of Health Sciences. **2016**;3:*79-82*.
6. Van Eerd LL, Hoagland RE, Zablotowicz RM, Hall JC. Pesticide metabolism in plants and microorganisms. Weed science. **200**3;51:*472-495*.
7. Gablenz S, Voltzke D, Abicht HP, Neumann-Zdralek J. Preparation of fine TiO_2 powders via spray hydrolysis of titanium tetraisopropoxide. Journal of materials science letters. **1998**;17: *537-539*.
8. Crooker SA, Awschalom DD, Baumberg JJ, Flack F, Samarth N. Optical spin resonance and transverse spin relaxation in magnetic semiconductor quantum wells. Physical Review B. **1997**;56:*7574*.
9. Li XZ, Li FB, Yang CL, Ge WK. Photocatalytic activity of WOx-TiO_2 under visible light irradiation. Journal of Photochemistry and Photobiology A: Chemistry. **2001**;141:*209-217*.
10. Zhang X, Thavasi V, Mhaisalkar SG, Ramakrishna S. Novel hollow mesoporous 1D TiO_2 nanofibers as photovoltaic and photocatalytic materials. Nanoscale. **2012**;4:*1707-1716*.
11. Zhou Y, Antonietti M. Synthesis of very small TiO_2 nanocrystals in a room-temperature ionic liquid and their self-assembly toward mesoporous spherical aggregates. Journal of the American Chemical Society. **2003**;125:*14960-14961*.
12. Gupta VK, Eren T, Atar N, Yola ML, Parlak C, Karimi-Maleh H. $CoFe_2O_4$@TiO_2 decorated reduced graphene oxide nanocomposite for photocatalytic degradation of chlorpyrifos. Journal of Molecular Liquids. **2015**;208:*122-129*.
13. Luo P, Zhang H, Liu L, Zhang Y, Deng J, Xu C, Hu N, Wang Y. Targeted synthesis of unique nickel sulfide (NiS, NiS_2) microarchitectures and the applications for the enhanced water splitting system. ACS applied materials & interfaces. **2017**;9:*2500-2508*.
14. Mitchell MF, Roberts JR. A case study of the use of fenitrothion in New Brunswick: The evolution of an ordered approach to ecological monitoring.Effects of pollutants at the ecosystem level. SCOPE. **1984**;22:*377-402*.
15. Zdravkov BD, Cermák JJ, Sefara M, Janku J. Pore classification in the characterization of porous materials: A perspective. Central European Journal of Chemistry. **2007**;5:*385-395*.
16. Thommes M, Kohn R, Fröba M. Sorption and pore condensation behavior of pure fluids in mesoporous MCM-48 silica, MCM-41 silica, SBA-15 silica and controlled-pore glass at temperatures above and below the bulk triple point. Applied surface science. **2002**;196:*239-249*.
17. Taguchi A, Schuth F. Ordered mesoporous materials in catalysis. Microporous and mesoporous materials. **2005**;77:*1-45*.

18. Fan XX, Yu T, Zhang LZ, Chen XY, Zou ZG. Photocatalytic degradation of acetaldehyde on mesoporous TiO_2: Effects of surface area and crystallinity on the photocatalytic activity. Chinese Journal of Chemical Physics. **2007**;20:*733-738*.

19. Kumar PV, Cheriyan VD, Seshadri M. Evaluation of spontaneous DNA damage in lymphocytes of healthy adult individuals from high-level natural radiation areas of Kerala in India. Radiation research. **2011**;177:*643-650*.

20. World Health Organization & United Nations Environment Programme. (1990). Public health impact of pesticides used in agriculture. Geneva: World Health Organization. http://www.who.int/iris/handle/10665/39772.

21. Sandeep S, Nagashree KL, Maiyalagan T, Keerthiga G. Photocatalytic degradation of 2, 4-dichlorophenoxyacetic acid-A comparative study in hydrothermal TiO_2 and commercial TiO_2. Applied Surface Science. **2018**;449:*371-379*.

22. Prieto F, Cortes S, Gaytan J, Ceruelos A, Vázquez P. Pesticides: Classification, Uses and Toxicity. Measures of Exposure and Genotoxic Risks.Journal of Research in Environmental Science and Toxicology. **2012**;1:*3-23*.

23. Son HK, Kim SA, Kang JH, Chang YS, Park SK, Lee SK, Jacobs Jr DR, Lee DH.Strong associations between low-dose organochlorine pesticides and type 2 diabetes in Korea. Environment international. **2010**;36:*410-414*.

24. Fromberg A, Granby K, Hojgard A, Fagt S, Larsen JC. Estimation of dietary intake of PCB and organochlorine pesticides for children and adults. Food Chemistry. **2011**;125:*1179-1187*.

25. Li H, Li J, Xu Q, Yang Z, Hu X. A derivative photoelectron chemical sensing platform for 4-nitrophenolate contained organophosphates pesticide based on carboxylatedperylene sensitized nano-TiO_2. Analyticachimicaacta. **2013**;766: *47-52*.

26. Sharma A, Mahajan VK, Mehta KS, Chauhan PS, Sharma V, Sharma A, Wadhwa D, Chauhan S. Pesticide contact dermatitis in agricultural workers of Himachal Pradesh (India). Contact dermatitis. **2018**;79:*213-217*.

27. Huang S, Chen C, Tsai H, Shaya J, Lu C. Photocatalytic degradation of thiobencarb by a visible light-driven MoS2 photocatalyst. Separation and Purification Technology. **2018**;197:*147-155*.

28. Nutter TJ, Jiang N, Cooper BY. Persistent Na^+ and K^+ channel dysfunctions after chronic exposure to insecticides and pyridostigmine bromide. Neurotoxicology. **2013**;39:*72-83*.

29. Chen J, Yao B, Li C, Shi G. An improved Hummers method for eco-friendly synthesis of graphene oxide. Carbon. **2013**;64:*225-229*.

30. Wang J, Zhou Y, Hu Y, O'Hayre R, Shao Z. Facile synthesis of nanocrystalline TiO_2 mesoporous microspheres for lithium-ion batteries. The Journal of Physical Chemistry C. **2011**;115:*2529-2536*.

31. Zhu J, Ren J, Huo Y, Bian Z, Li H. Nanocrystalline Fe/TiO_2 visible photocatalyst with a mesoporous structure prepared via a nonhydrolytic sol- gel route. The Journal of Physical Chemistry C. **2007**;111:*18965-18969*.

32. Kumar KV, Porkodi K, Rocha F. Langmuir-Hinshelwood kinetics–a theoretical study. Catalysis Communications. **2008**;9:*82-84*.